SUBJECT AREAS

Optics and photonics, material science, physics, solar cells, electrical and electronic engineering, and optical materials and devices

Title:

Probing carrier lifetimes in photovoltaic materials using subsurface two-photon microscopy

Authors

Edward S. Barnard[1,2 *], Eric T. Hoke[2], Stephen T. Connor[2], James R. Groves[2], Tevye Kuykendall[1], Zewu Yan[3], Eric C. Samulon[3], Edith D. Bourret-Courchesne[3], Shaul Aloni[1], P. James Schuck[1 *], Craig H. Peters[2], Brian E. Hardin[2]

Affiliations

[1] The Molecular Foundry, Lawrence Berkeley National Laboratory, Berkeley CA

[2] PLANT PV Inc. Oakland CA

[3] Materials Sciences Division, Lawrence Berkeley National Laboratory, Berkeley CA

[*] Corresponding Authors: esbarnard@lbl.gov, pjschuck@lbl.gov

Abstract

Accurately measuring the bulk minority carrier lifetime is one of the greatest challenges in evaluating photoactive materials used in photovoltaic cells. One-photon time-resolved photoluminescence decay measurements are commonly used to measure lifetimes of direct bandgap materials. However, because the incident photons have energies higher than the bandgap of the semiconductor, most carriers are generated close to the surface, where surface defects cause inaccurate lifetime measurements. Here we show that two-photon absorption permits sub-surface optical excitation, which allows us to decouple surface and bulk recombination processes even in unpassivated samples. Thus with two-

photon microscopy we probe the bulk minority carrier lifetime of photovoltaic semiconductors. We demonstrate how the traditional one-photon technique can underestimate the bulk lifetime in a CdTe crystal by 10x and show that two-photon excitation more accurately measures the bulk lifetime. Finally, we generate multi-dimensional spatial maps of optoelectronic properties in the bulk of these materials using two-photon excitation.

Introduction

The minority carrier lifetime is considered the most critical and variable parameter in photovoltaic (PV) materials, and is a key determining factor of a device's open-circuit voltage[1,2] Well-established photoconductivity techniques (e.g. quasi-steady state photoconductivity) are often used to determine the minority carrier lifetimes for indirect bandgap materials, such as silicon, that have longer minority carrier lifetimes (20 μs – 1 ms).[3] However, these techniques are not effective at measuring the minority carrier lifetimes of direct bandgap materials, which typically range from 500 ps to 100 ns, or materials that have many traps and low doping levels.[4] For direct bandgap materials, optical techniques such as one-photon time-resolved photoluminescence (TRPL) are often used to estimate the minority carrier lifetime.[5]

In one-photon TRPL (1P-TRPL) measurements a short laser pulse (100 fs – 100 ps) impinges on a semiconductor of interest. The photons in the laser pulse have energies above the bandgap, so they are absorbed by the semiconductor and generate excess charge carriers. A fraction of these carriers radiatively recombine, emitting photons that are detected by a time-correlated single photon counting system. The photoluminescence (PL) decay transients generally provide a direct measure of the recombination dynamics, and thus can be used to determine the minority carrier lifetime. In these measurements the absorption of the excitation pulse follows an exponential absorption profile (Beer's law), which results in the majority of excess carriers being generated typically within 100-500 nm of the semiconductor surface, as shown in Fig. 1a.

For material systems with a low surface recombination velocity (SRV), surface effects are minimal and the bulk minority carrier lifetime can be accurately determined by measuring a monoexponential TRPL decay.[6] However, many PV material systems have a large SRV, which limits the lifetime of carriers generated near the surface.[6,7] A stark example of the effect of SRV on measured lifetime is the work by Metzger et al. that showed that a $Cu(In,Ga)Se_2$ (CIGS) film's exposure to air resulted in 1P-TRPL lifetimes changing by a factor of 50x.[8] Because of the strong effect of surface recombination in optical measurements, it is desirable to develop methods to separate surface and bulk lifetimes. One method used to probe surface and bulk recombination dynamics in silicon devices is to utilize the wavelength-dependent absorption depth and measure TRPL decay dynamics at different excitation wavelengths.[9] However, this technique becomes more challenging to use with direct bandgap thin film materials, which have absorption coefficients that are 10-100x larger than silicon.

Measuring the bulk properties of semiconductors more accurately therefore requires developing new experimental techniques to mitigate effects from the surface of the semiconductor films. Surface passivation is a common approach for reducing surface defects[6] that can reduce the SRV and allow the direct measurement of minority carrier lifetimes[10]. Such surface passivation techniques have been well-studied for some conventional PV semiconductors such as GaAs and CIGS, but are not ideal because additional surface preparation and deposition steps are required. Additionally, surface passivation methods are not well established for many other thin film semiconductors, making optical determination of bulk charge carrier lifetimes problematic. Polycrystalline CdTe is an important example where a $CdCl_2$ passivation technique exists, but its effects are not solely limited to the surface of the CdTe film.[11] It is therefore desirable to develop a characterization technique that decouples surface and bulk recombination processes while eliminating the challenges associated with surface passivation. We show that using two-photon (2P) excitation, we can optically excite carriers at specific locations within a sample to avoid surface effects.

The operating principle (and primary advantage) of 2P microscopy is that the location of absorption can be controlled by laser intensity. Thus by shaping and focusing the laser beam it is possible to excite carriers many microns below the surface of a sample. Unlike

one-photon (1P) experiments, which use photons with energies above the bandgap, two-photon measurements use photons with sub-bandgap energies. As a result, carriers can be excited only if the material absorbs multiple photons simultaneously – a process that is non-linearly proportional to the local incident photon flux. As illustrated by Fig. 1b, in a confocal microscope most of the laser intensity is concentrated in the focal volume, leading to high 2P absorption only within this region.[12] It is possible to move the position of the focal volume throughout the sample by moving the sample relative to the confocal microscope. While the selection rules of 1P and 2P absorption are, in-principle, different, the dynamics of recombination and re-emission are identical. Thus for well-passivated systems the 1P and 2P luminescence lifetimes are similar because the system relaxes to the same excited state before recombination occurs in both cases.[13] This equivalence allows us to use 2P excitation to replace and extend 1P excitation for carrier lifetime measurements. 2P excitation additionally allows us to peer below the surface and investigate carrier dynamics where 1P excitation cannot probe.

Due to the ability to probe below the surface of a sample, 2P microscopy has been extensively used for biological applications.[14] Recently, 2P microscopy has also seen preliminary use in the analysis of semiconducting materials and devices. For example, Jursenas et al. performed both 1P and 2P TRPL on GaN and showed that 2P can probe below the surface of a semiconductor.[15] However their use of an unfocused, weakly absorbed beam, did not allow for depth resolution. Schuck et al. used a confocal microscope and continuous wave laser to perform depth-resolved 2P excitation to probe the photoluminescence spectra of thick GaN samples for light emitting diode applications, with a depth resolution of 1.75 μm.[16]

In this paper we show that 2P excitation can now be combined with time-resolved photoluminescence (2P-TRPL) to measure the charge carrier lifetime inside the semiconductor, removing the primary limitation of 1P-TRPL. We use 2P excitation to study the minority carrier lifetimes of PV materials and demonstrate the first use of depth-of-focus, 2P-TRPL for PV. This work shows how this method can be used to limit the effects of surface recombination and study the bulk properties more directly in a CdTe model system. CdTe is studied because a better understanding of its bulk minority charge carrier lifetime has the potential to dramatically improve device performance; it is

hypothesized that the large deviation from the ideal efficiency in CdTe solar cells is attributed to low carrier lifetime (i.e. ≤ 3 ns as measured by 1P-TRPL).[5] Our work also lays the foundation for determining the resolution limit for depth-of-focus 2P-TRPL experiments. We additionally show how this technique can be extended to multi-dimensional mapping of optoelectronic properties in semiconductor crystals and thin films.

Results

Description of the two-photon microscopy system

The 2P-TRPL system consists of a pulsed near-infrared (NIR) Ti:Sapphire laser that is coupled to a confocal microscope with a dichroic beam splitter and an objective lens that focuses the light onto the sample, as shown schematically in Fig. 2a. In this system, sub-bandgap NIR light excites carriers in the semiconductor within the focal volume via 2P absorption (red lines). The photo-generated excess carriers radiatively recombine, emitting photons through the objective lens (green lines) that are collected confocally by an avalanche photodetector and recorded by time-correlated single-photon counting electronics. The sample is mounted on a three-axis stage, which allows the excitation volume to be moved both laterally across the film and into the depth of the film, thus permitting tomographic mapping of optoelectronic properties.

To verify that 2P absorption was occurring in each of our test samples, the photoluminescence intensity was measured as a function of the excitation intensity. As a model system, we measured the PL intensity dependence for solutions of the organic dye Rhodamine 101 in ethanol, which is known to have a PL quantum efficiency of nearly 100%.[17] When excited with below bandgap light (λ=830nm), the photoluminescence intensity was proportional to the square of the laser fluence (power law of 1.93). Conversely, when excited by above bandgap light, the photoluminescence intensity was linearly proportional to the fluence (power law of 1.05) (see Fig. 2b).

Demonstrating depth-of-focus two-photon microscopy

The depth-of-focus resolution of the 2P excitation is important in determining the spatial limitations of the technique. Most thin film absorbers used for PV applications are 2–7 μm in thickness, thus a depth resolution on this order is required. In practice, subsurface depth resolution depends significantly on the imaging optics, and is influenced by factors such as the use of immersion lenses and aberration corrected optics. In order to test the depth resolution of the 2P excitation microscope, a double InGaN/GaN/InGaN quantum well (QW) stack (Fig. 3a) was fabricated to demonstrate that the emission of the two quantum well layers could be separated. The structure was grown on a sapphire substrate using MOCVD and the In/Ga ratio was adjusted between the top and bottom quantum wells in order to shift the emission for the two QW layers to 430 nm and 460 nm, respectively. The QWs were separated by a 3 μm-thick layer of GaN. The 3 μm separation distance between QW layers was measured by in-situ interferometry and confirmed using cross-sectional cathodoluminscence (Fig. 3b).

It is important to note that the index of refraction of GaN (n=2.35 in the near-infrared region) is comparable to many semiconductors of interest, so similar resolution can be expected for other photovoltaic materials. For this quantum well structure we predict a FWHM diffraction-limited, aberration-free axial (depth) resolution of 1.7 μm for an excitation wavelength of 830 nm and emission wavelength of 460 nm (see supporting information). However, in practice the depth-of-focus increases as the focal volume is focused deeper into the sample due to aberrations caused by refraction at the surface of the sample.[17]

Experimentally the excitation volume was first focused above the surface of the sample and subsequently moved into the sample in step sizes of 100 nm, while rastering laterally. PL spectra were collected at each point using a spectrometer to create a hyperspectral depth profile of the PL. In order to delineate the emission from the two QWs and exclude PL from GaN defects we integrated the PL emission within a 30 nm band around the central emission peak for each QW, as shown in Figs. 3c and 3d. Figures 3e and 3f show the integrated PL from each band as a function of the nominal focus distance (relative sample stage movement) into the structure. Two distinct regions of high fluorescence are observed corresponding to the two quantum well layers.

We note that the actual focal depth in the sample is larger than the nominal focus depth defined by the sample stage movement. This is due to refraction at the air-sample interface.[17] Consequently the location of the emission peaks from the two quantum well structures are separated by a scan distance (nominal focus depth) of only 2.0 μm despite being physically separated by 3.0 μm. Figure 3g plots the intensity as a function of depth for the upper (blue) and lower (red) QWs. The peaks for each QW are clearly visible. The region in between the two QWs displays a plateau in the PL, which is caused by spectral overlap of the two QW emission spectra. This result shows that with 2P absorption we are able to excite and collect PL from a layer in the sample 3 μm below the surface.

Comparing 1P and 2P TRPL transients of CdTe crystals

CdTe single crystal samples (110-oriented) were used to compare conventional 1P-TRPL with 2P-TRPL measurements. With CdTe we demonstrate the ability of 2P-TRPL to decrease the effects of surface recombination on measured carrier lifetimes of a PV material. The CdTe crystals are considered intrinsic with a resistivity between 10^6-10^8 Ω cm and carrier concentration of less than 10^{10} cm^{-3}. The crystals were polished to a mirror finish, which results in a large density of defects at the surface and thus a high surface recombination velocity.

In the first series of experiments, the CdTe crystal was studied as received without any chemical modifications. The untreated CdTe crystal's carrier lifetime was measured with 1P-TRPL using a 485 nm pulsed diode laser with a 100 ps pulse width and pulse energy of ~4pJ/pulse. This corresponds to an estimated excess carrier density of ~10^{19} cm^{-3}. The 1P-TRPL transients were independent of the excitation intensity around this fluence level, indicating that Auger recombination is not significant under these excitation conditions. PL was collected by an avalanche photodiode coupled to a monochromator set at 820 nm. The resulting time trace is plotted in Fig. 4 (blue) and is well described by a monoexponential decay with a short 0.34 ns lifetime.

The lifetime obtained by 1P-TRPL is lower than expected for a single crystal and is likely dominated by defect recombination at and near the surface due to damage induced during the polishing process.[18,19] One method commonly used to measure defect densities in thin films is cathodoluminscence (CL).[20] CL measurements produce high-

resolution maps of areas of increased or reduced photoemission that do not necessarily correlate with topography or other secondary electron emission contrast. Regions of higher defect densities produce lower CL signal and can thus be mapped across a sample surface. The resolution of this technique is often high enough to see individual defect recombination centers. Figures 5a and 5b show the SEM and CL images, respectively, of the surface of the CdTe crystal. From Fig. 5b we see a large number of defects at the surface, which are visible as white spots in the reverse contrast CL image. From the CL image we estimate an areal defect density of at least 10^8 cm^{-2}.

2P-TRPL was then used to decouple the effects of surface and bulk recombination on measured carrier lifetime on this untreated CdTe crystal. In this experiment pulsed infrared (920 nm) light from a Ti:Sapphire laser (150 fs pulse width) was passed through a confocal microscope in order to induce 2P absorption in the crystal within a diffraction limited focal volume of approximately 1 μm^3. To verify 2P absorption in CdTe we performed a power dependent PL measurement. We obtained a power-dependence that was super-quadratic and saturated at larger fluences (see supporting information). We attribute the super-quadratic power response of this 2P process to the presence of multiple recombination channels through either free and bound excitons, or trapped donor and acceptor sites.[21] A pulse energy of 4 pJ/pulse was chosen for the subsequent experiments. This corresponds to an estimated maximum excess carrier density of 10^{18} cm^{-3}.

When the 2P excitation was focused at the top of the untreated CdTe sample to generate charge carriers primarily at the surface, a PL decay transient was observed (Fig. 4, green) that is similar to the decay dynamics observed with 1P excitation (Fig. 4, blue). This suggests that in the 1P-TRPL measurements the photons are strongly absorbed near the surface, generating charges only in the highly defective near-surface region. A biexponential fit of this surface 2P data is dominated by a 0.25 ns lifetime component with a smaller contribution from a 0.73 ns slower component, and is similar to the rapid 0.34 ns decay observed from 1P-TRPL. We note that although similar surface lifetimes were measured via 1P- and 2P-TRPL, a direct correspondence between the two excitation methods is not necessarily expected due to differences in excitation volume between 1P and 2P.

When the untreated CdTe sample was moved 3 μm towards the objective there was an increase in both lifetimes obtained from a biexponential fit (Fig. 4, red). The fast component increased to a 0.49 ns lifetime, while the longer lifetime component lengthened to 1.8 ns, which is a 2.5x increase compared to the lifetime measured near the surface of the crystal. This increase in lifetime can be attributed to the photoexcitation of only the bulk region within the CdTe crystal where the lifetime is not limited by surface defects.

2P-TRPL depth profiling of a CdTe Crystal

To observe the transition region from surface to bulk-dominated recombination, the untreated CdTe single crystal sample was probed with 2P-TRPL as a function of depth. The laser excitation volume was focused above the sample surface and subsequently moved into the crystal to a nominal focus depth of 5 μm in 200 nm steps. At each depth a time trace of PL was collected and the fast and slow components of the decay were extracted using a biexponential fit. The surface of the sample was assumed to be at the depth where the PL lifetime reached a minimum. Figure 6a shows the PL intensity as a function of nominal focus depth. The PL intensity first increases as the whole focal volume is pushed into the sample and then declines due to both reabsorption of the emitted light and optical aberrations from refraction at the top of the sample. These aberrations cause the depth and size of the focal volume to increase linearly as the focus is moved further into the sample,[17] and practically limit the maximum depth with a large (> 0.8) numerical aperture objective lens used in air to less than 10 μm in materials with a similar index of refraction ($n_{\mathrm{CdTe}} \sim 3$). This can be improved significantly with the use of immersion optics.

Figures 6b and 6c show the fast (τ_f) and slow (τ_s) lifetime components, respectively, extracted from a biexponential fit as a function of nominal focus depth (Δz). Error bars indicate standard deviation of fits from repeated depth scans. The fast and slow lifetimes are shortest very close to the CdTe surface and increase by a factor of 1.8x and 2.5x, respectively, as the excitation volume is pushed further into the sample. Figure 6e shows 2P-TRPL decay curves at three representative nominal depths: at the surface

($\Delta z = 0$ µm, $\tau_s = 0.73$ ns), within the transition region ($\Delta z = 1.0$ µm, $\tau_s = 1.2$ ns), and below the transition region ($\Delta z = 4.5$ µm, $\tau_s = 1.8$ ns). Figure 6d shows the weighting of the fast and slow components of the biexponential fit. The lifetimes both plateau at nominal focus depths greater than 3 µm into the crystal, which suggests that the excitation volume has moved far enough away from the surface that surface effects are no longer important. However, it is clear that there continues to be a fast and slow component to the decay profile even as the excitation volume is pushed deep into the bulk where surface effects have been removed. This continued multi-exponential decay behavior indicates that there are multiple decay pathways in the bulk with a fast, sub-nanosecond component still being the dominant contributor to bulk recombination.

Identifying the origins of low lifetimes in the untreated CdTe crystal

The multi-exponential, < 2 ns bulk lifetime of the untreated CdTe crystal indicates that there are many processes that limit the carrier lifetime. In general, CdTe single crystals can display a large range in bulk charge carrier lifetimes due to variations in crystal quality.[22] Point defects, such as vacancies, as well as extended defects, such as threading dislocations, can act as charge carrier recombination centers and thus lower the carrier lifetime in the crystal.[1,23] In order to understand the limiting defects in the sample, the untreated CdTe crystal was cleaved and the resulting cross-sectional region was examined using CL to study the structural defects in the bulk. Figures 5c and 5d show the cross-sectional SEM and CL images of the sample. The defects are visible in the CL image as white spots. We estimate the areal defect density in the bulk to be 10^6 cm^{-3}. A visual comparison of the CL images from the surface (Fig. 5b) and bulk (Fig. 5d) provides evidence for a significantly reduced number of defects in the bulk of the crystal, which is partly responsible for the increase in the lifetime. Interestingly, while the defect densities of the surface and bulk of the untreated CdTe crystal were ~10^6 cm^{-2} and ~10^8 cm^{-2}, respectively, the lifetimes differed by only a factor of ~2.5x. Yamaguchi et al. developed an approximation to determine the impact of the defect density on the minority carrier lifetime of single crystals based on the ambipolar diffusivity and threading dislocation density.[24 25] Assuming that the observed defects were threading dislocations

and an ambipolar diffusivity for CdTe of between 2–10 cm^2/Vs we would expect the charge carrier lifetimes from the surface and bulk of the CdTe crystal to differ by up to 100x, which is substantially different from that seen with the untreated CdTe crystal. This implies that the defects seen in CL are not the limiting recombination pathway in the bulk CdTe crystal.

Previously, researchers have studied point defects in CdTe and CdZnTe crystals and have identified cadmium vacancies as deep level traps.[26] Such vacancies are not visible in CL imaging. CdTe crystals are often grown under Te rich conditions or have impurities added (e.g., In) that act as compensating defects to make highly resistive substrates for detector applications. The compensating defects can dramatically reduce the minority carrier lifetime. Rosenwaks et al. have reported significantly higher (180 ns) minority carrier lifetimes when treating intrinsic CdTe crystals in a Cd and In overpressure[22] and annealing CdTe crystals in a Cd overpressure has previously been shown to change the doping density and type, which was attributed to the reduction of Cd vacancies.[27]

Using 2P-TRPL to Measure CdTe crystal carrier lifetime improvements through Cd overpressure

In an effort to increase the bulk carrier lifetime of the sample we annealed the same CdTe crystal measured in Figs 4-7 in a Cd overpressure environment. The crystal was placed in a quartz ampoule that contained a piece of Cd shot and was evacuated to 10^{-5} torr and subsequently sealed. The CdTe crystal was then heated to 500°C for 24 hours in the ampoule and cooled over five hours. Depth-of-focus 2P-TRPL, shown in Fig. 7, was performed on the treated CdTe crystal and revealed a >10x increase in the bulk lifetime over the untreated sample. The resulting components of the biexponetial fit of the lifetime curves are shown in Fig 7b (fast) and Fig. 7c (slow component). The weightings for the fast and slow components are shown in Fig. 7d and reveal a clear transition from short, surface-dominated to long, bulk-dominated recombination dynamics. This clear transition was not observed in the sample prior to this Cd treatment. The weighting for the slow

component in the bulk approaches unity, indicating there is now a single dominant decay pathway in the bulk that results in a monoexponential decay.

At the surface, the 2P TRPL decay of the treated CdTe crystal is dominated by a fast component with a lifetime of 0.23 ns, which is similar to the fast component before treatment. This suggests that the treatment left the surface unimproved. There is however a small contribution of a 9 ns slow component, which is much longer than the untreated sample's 0.7 ns. At a nominal focus depth of 1 μm we find that the fast (τ_f = 0.45 ns) and slow (τ_s = 17.6 ns) components are equally weighted. Deeper in the sample, the slow component dominates and reaches a τ_s = 73.0 ns at a nominal focus depth of 3.4 μm. At depths below this we note a continued increase in lifetime but we are unable to quantify this due to a limited 12 ns time window defined by the laser repetition rate. The slow components in these measurements are an order-of-magnitude longer than the equivalent measurements done on the untreated sample, indicating an improvement in bulk carrier lifetime due to the Cd treatment.

We also performed 1P TRPL on this annealed sample (Fig. 7e). The 1P decay is strongly dominated by a 0.5 ns component with a small contribution from a 5 ns long tail. We note that the 5 ns tail from 1P is shorter and less prevalent than the 9 ns tail from 2P-TRPL at the surface. This difference can again be attributed to difference excitation volumes between 1P and 2P excitation. However neither 1P nor 2P surface measurements show the >70 ns bulk lifetime revealed by the sub-surface 2P measurement.

Mapping PL and charge carrier lifetime in two dimensions

Two-photon excitation is not only a powerful tool to decouple surface and bulk processes but also can be used for mapping inhomogeneities within a sample with high spatial resolution. This can be used to identify defective regions with reduced lifetimes as well as probe buried features or interfaces. In addition to depth variations, we also measured lateral variations of carrier lifetimes in the untreated CdTe crystal, as shown in Fig. 8. A two-dimensional map of PL and charge carrier lifetimes in the untreated CdTe crystal was generated by rastering the 2P excitation volume across the sample with a 250 nm

lateral step size and a 100 nm step size into the film. TRPL measurements were collected at each point and the fast and slow components were extracted, as previously described. Figure 8a shows the integrated PL for each data point in the region that was examined. Lateral variability of about 15% is seen across the sample near the surface, which may be due to changes in the rate of recombination or variations with in- or out-coupling of light due to surface features (e.g., polishing induced scratches). Figures 8b and 8c show the fast and slow lifetimes at each point in the sampled region. There is a clear trend toward increasing lifetime for both the fast and slow decay components at increased depths in the film. However, there is also lateral variability at $\Delta z = 1$ μm with the left region of the sample showing on average shorter lifetimes for both the fast and slow components (1.2 ns on the left versus 1.5 ns on the right). This is not explained by the small variations in absorption or out-coupling of light and is likely due to variations in the defect density in the two parts of the sample.

It is important to note that finer grained inhomogeneities (pixel-to-pixel) in the lifetime fits can be attributed to the limited number of photons collected at each pixel. Shot noise becomes problematic as the excitation is pushed deeper into the film since we are collecting only 10^4 photons per pixel near the bottom of the scan. This can lead to a lower signal-to-noise ratio and a less accurate fit, illustrating the trade-off of acquisition time, spatial resolution, and confidence of lifetime measurements.

Discussion

There are important insights gained by comparing 1P-TRPL and depth-of-focus 2P-TRPL results as summarized in Table 1. Traditionally, the bulk minority carrier lifetime has been estimated from the long tail in 1P-TRPL measurements.[28] However, we find that the long tail from 1P-TRPL does not accurately measure the bulk lifetime for unpassivated crystals. This applies in the both the extreme cases of the untreated (short lifetime) and treated (long lifetime) CdTe crystal. 1P-TRPL on the Cd-treated CdTe crystal show a slow lifetime component of 5 ns, which is a factor of >10x lower than the bulk lifetime measured using 2P-TRPL (5 ns vs. > 70 ns). For untreated CdTe, only a

sub-nanosecond lifetime could be measured using 1P-TRPL while 2P-TRPL revealed a 2.5 ns component within the bulk of the material. These results clearly show that high surface recombination velocities greatly distort the 1P-excited carrier dynamics and great care should be taken when assigning the slow decay component to the actual bulk lifetime, especially with unpassivated samples.

While sub-surface 2P-TRPL of the treated CdTe crystal showed monoexponential decay (τ_s = 73 ns with 96% weighting), the sub-surface 2P-TRPL of the untreated CdTe crystal film continued to exhibit a multi-exponential decay that is mainly weighted toward the fast component at similar depths (τ_f = 0.49 (78%) versus τ_s = 1.82 (22%)) . Given that the excitation volume is far away from the surface, it is highly likely that multiple recombination pathways in the bulk contribute the multi-exponential bulk carrier lifetime. While the Cd treatment was able to ameliorate the defects in the bulk of the CdTe crystal without directly identifying the defect mechanism, we anticipate the need to directly identify the character and mechanism of performance-degrading defects. Thus low-temperature, sub-surface 2P photoluminescence measurements may be a useful tool to directly identify bulk defects for other CdTe morphologies or other material systems.

In the present study CdTe single crystals with a moderate density of structural defects (i.e. 10^6 cm^{-2}) were shown to obtain relatively high minority carrier lifetimes when annealed in a Cd-rich atmosphere, likely due to the filling of Cd vacancies. Moving forward, one of the greatest challenges in studying thin film solar cells is determining which defect types (e.g. grain boundaries, intragrain structural defects, point defects, etc.) are responsible for low lifetimes. Future studies of 2P-TRPL mapping coupled with structural analysis on poly-crystalline CdTe films may elucidate the connection between structure (grain size, grain boundary angles and intragrain defects), local carrier lifetime, and ultimately device performance.

Understanding the spatial resolution of 2P excitation is important in order to determine the applicability of 2P-TRPL to thin films. In this work it was shown that the charge carrier lifetime increased as the excitation was pushed into the CdTe crystal and saturated at some depth below the surface. This indicates that 2P excitation can be a powerful tool to decouple surface and bulk effects. In addition, we were able to resolve

InGaN QWs that were separated by 3 μm by spectrally separating their emission. This is evidence for the ability to distinguish surface and buried features. However, it should be noted that attempts to resolve the InGaN QWs by measuring total PL intensity across all wavelengths as a function of depth were less successful. Emission from defect states in the 3 μm-thick GaN layer between the wells and lower out-coupling of emission from the buried QW led to less defined peaks for each of the QWs. Further studies are being performed on structures that are separated by non-emissive layers that should shed further light on the experimentally achievable spatial resolution of the 2P excitation technique. In addition, in order to reconstruct accurate spatial maps involving depth profiling, the apparent depth from stage movement needs to be converted into the actual focal depth.[17] Further characterization of the optical system is required to accurately apply such a correction.

In samples where higher resolution is required, the use of a solid immersion lens can substantially improve the spatial resolution and reduce aberrations occurring due to refraction at the top of the sample.[29,30] It is important to ensure that the index of refraction of the solid immersion lens matches the substrate index to maximize the resolution of the system. However, the use of a solid immersion lens limits the lateral scanning capabilities and therefore the extent to which mapping can be performed. Oil immersion lenses have the potential to be optimal for most 2P-TRPL studies, with improved resolution over air-objectives and no scanning range limits as in the case of solid immersion lenses. However typical oil-immersion optics show unacceptable aberrations when used with non-index matched samples.[31]

Two-photon excitation is a powerful tool to allow multi-dimensional mapping of the optoelectronic properties of thin film PV materials. Although this study examined the PL and charge carrier lifetime of single crystal CdTe, it is highly desirable to apply this technique to the study of polycrystalline thin films of CdTe and CIGS. Creating PL and lifetime maps of CdTe/CdS films should provide insight into the extent to which sulfur diffusion occurs into the bulk from the CdS interface and to what extent the lifetime correlates with sulfur concentration. In the case of CIGS, 3D PL and lifetime maps can shed light onto the effects of grading the Ga concentration in the CIGS film and help

identify compositional and lifetime inhomogeneities both laterally and as a function of depth. Since this a general technique, we additionally foresee 2P microscopy as a tool in the development of many other novel PV materials.

Methods

Samples: Rhodamine 101 was diluted in ethanol to a concentration of $2x10^{-4}$ M and placed in a cuvette. For the 2P measurement a 10x objective was used to allow for a greater working distance required by using a cuvette. The InGaN quantum well sample was grown using MOCVD on a C-plane sapphire substrate using a Thomas Swan 2x3 close-coupled showerhead reactor. Trimethylgallium, trimethylindium and ammonia where used as Ga, In and N precursors, respectively. Two sets of five 2.5 nm-thick InGaN quantum wells, with 7 nm GaN barriers were grown on top of a 2 µm-thick GaN buffer and separated by a 3 µm-thick GaN layer and capped by 300 nm-thick GaN layer. The emission wavelength of the QWs was tuned to ~430 nm and ~460 nm by changing the indium concentration through varying the growth temperature between 750 and 720°C, respectively. Bridgeman grown, CdTe (110) single crystals were obtained from MTI Corp. The crystals were polished to a mirror finish as received. The CdTe crystals were subsequently annealed with a piece of Cd shot in an evacuated (10^{-5} Torr) quartz ampoule for 24 hours at 500°C and finally cooled for 5 hours.

One-Photon Time-resolved Photoluminescence. Samples were excited with a pulsed laser diode, (PicoQuant LDH 485 nm, 100 ps FWHM pulse duration, 10 MHz) focused with a 10x NA=0.25 objective, spectrally filtered using an Acton 2300i spectrometer and detected with a single-photon avalanche diode (Micro Photon Devices PDM series). A PicoQuant PicoHarp 300 time-correlated single-photon counting (TCSPC) system was used to record the timing data.

Two-Photon Time-resolved Photoluminescence. A confocal microscope system was constructed using a Nikon Eclipse Ti-U microscope with a Nikon 100x NA=0.95 NA objective and a three axis MadCityLabs NanoPDQ piezo nanopositioning sample stage. A Coherent Mira 900 Ti:Sapphire excitation laser (700-1000 nm tunable, 150 fs pulse

duration, 80MHz) is optically coupled to the input of the microscope. The laser was tuned to 830 nm for the InGaN quantum well and Rhodamine 101 samples and was tuned to 920 nm for the CdTe sample. Photoluminescence was collected through a 150 μm pinhole and into detection optics. For spectral collection we used and Acton 2300i spectrometer with 150 groves/mm grating and an Andor iXon electron-multiplied CCD. For time-resolved collection we first spectrally-filtered the PL using band pass filters and then collected with a single-photon avalanche diode (Micro Photon Devices PDM series). A PicoQuant PicoHarp 300 time-correlated single-photon counting (TCSPC) system was used to record the timing data. Lifetimes were fit to a biexponential decay using a constrained least-squared algorithm. A laser pulse energy of 4pJ/pulse was used to excite the CdTe sample.

Cathodoluminescence Microscopy. We performed CL measurements in a Zeiss Gemini Supra 55 scanning electron microscope at 15kV. CL emission was collected via a multimode optical fiber positioned 300 μm away from the electron-beam location on the sample. CL was then spectrally filtered with an Acton 2300i spectrometer. For CL images collected in a narrow spectral bandwidth, the photons were collected by either a Hamamatsu 7360-01 photomultiplier tube or a Perkin-Elmer SPCM-AGR-15 silicon-avalanche photodiode (below and above 530 nm, respectively).

1. Green, M. A. *Solar cells: Operating principles, technology, and system applications*. (Prentice-Hall, Inc., 1982).
2. Ahrenkiel, R. K. Measurement of minority-carrier lifetime by time-resolved photoluminescence. *Solid-State Electronics* **35,** 239–250 (1992).
3. Sinton, R. A., Cuevas, A. & Stuckings, M. Quasi-steady-state photoconductance, a new method for solar cell material and device characterization. *IEEE Phot. Spec. Conf.* 457–460 (1996). doi:10.1109/PVSC.1996.564042
4. Ahrenkiel, R. K., Call, N., Johnston, S. W. & Metzger, W. K. Comparison of techniques for measuring carrier lifetime in thin-film and multicrystalline photovoltaic materials. *Sol. Energ. Mat. Sol.* **94,** 2197–2204 (2010).

5. Metzger, W. K. *et al.* Time-resolved photoluminescence studies of CdTe solar cells. *J. Appl. Phys.* **94,** 3549–3555 (2003).
6. Nelson, R. J. & Sobers, R. G. Minority-carrier lifetimes and internal quantum efficiency of surface-free GaAs. *J. Appl. Phys.* **49,** 6103–6108 (1978).
7. Ahrenkiel, R. K. *et al.* Ultralong minority-carrier lifetime epitaxial GaAs by photon recycling. *Appl. Phys. Lett.* **55,** 1088–1090 (1989).
8. Metzger, W. K., Repins, I. L. & Contreras, M. A. Long lifetimes in high-efficiency $Cu(In,Ga)Se_2$ solar cells. *Appl. Phys. Lett.* **93,** 022110 (2008).
9. Ahrenkiel, R. K. & Johnston, S. W. An optical technique for measuring surface recombination velocity. *Sol. Energ. Mat. Sol.* **93,** 645–649 (2009).
10. Shimakawa, S. *et al.* Characterization of Cu(In,Ga)Se2 thin films by time-resolved photoluminescence. *Phys. status solidi (a)* **203,** 2630–2633 (2006).
11. McCandless, B. E. & Sites, J. R. in *Handbook of Photovoltaic Science and Engineering* (Luque, A. & Hegedus, S.) 617–662 (John Wiley & Sons, Ltd, 2005).
12. Denk, W., Strickler, J. & Webb, W. Two-photon laser scanning fluorescence microscopy. *Science* **248,** 73 –76 (1990).
13. Schuck, P. J., Willets, K. A., Fromm, D. P., Twieg, R. J. & Moerner, W. E. A novel fluorophore for two-photon-excited single-molecule fluorescence. *Chem. Phys.* **318,** 7–11 (2005).
14. Helmchen, F. & Denk, W. Deep tissue two-photon microscopy. *Nat. Meth.* **2,** 932–940 (2005).
15. Jursenas, S. *et al.* Carrier recombination and diffusion in GaN revealed by transient luminescence under one-photon and two-photon excitations. *Appl. Phys. Lett.* **89,** 172119–172119–3 (2006).
16. Schuck, P. J., Grober, R. D., Roskowski, A. M., Einfeldt, S. & Davis, R. F. Cross-sectional imaging of pendeo-epitaxial GaN using continuous-wave two-photon microphotoluminescence. *Appl. Phys. Lett.* **81,** 1984–1986 (2002).
17. Everall, N. J. Modeling and Measuring the Effect of Refraction on the Depth Resolution of Confocal Raman Microscopy. *Appl. Spectrosc.* **54,** 773–782 (2000).
18. Kosyachenko, L. A., Sklyarchuk, V. M., Sklyarchuk, Y. F. & Ulyanitsky, K. S. Surface-barrier p-CdTe-based photodiodes. *Semicond. Sci. Technol.* **14,** 373 (1999).
19. Rosenwaks, Y., Shapira, Y. & Huppert, D. Picosecond time-resolved luminescence studies of surface and bulk recombination processes in InP. *Phys. Rev. B* **45,** 9108–9119 (1992).
20. Lu, H. *et al.* Cathodoluminescence mapping and selective etching of defects in bulk GaN. *J. Cryst. Growth* **291,** 82–85 (2006).
21. Schmidt, T., Lischka, K. & Zulehner, W. Excitation-power dependence of the near-band-edge photoluminescence of semiconductors. *Phys. Rev. B* **45,** 8989–8994 (1992).
22. Cohen, R., Lyahovitskaya, V., Poles, E., Liu, A. & Rosenwaks, Y. Unusually low surface recombination and long bulk lifetime in n-CdTe single crystals. *Appl. Phys. Lett.* **73,** 1400 (1998).
23. Fahrenbruch, A. & Bube, R. H. *Fundamentals of solar cells*. (Academic Press,Orlando, FL, USA, 1983).
24. Yamaguchi, M. & Amano, C. Efficiency calculations of thin-film GaAs solar cells on Si substrates. *J. Appl. Phys.* **58,** 3601–3606 (1985).

25. Ahrenkiel, R. K. *et al.* Minority Carrier Lifetime of GaAs on Silicon. *J. Electrochem. Soc.* **137,** 996–1000 (1990).
26. Castaldini, A., Cavallini, A., Fraboni, B., Fernandez, P. & Piqueras, J. Deep energy levels in CdTe and CdZnTe. *Journal of Applied Physics* **83,** 2121–2126 (1998).
27. Lyahovitskaya, V., Chernyak, L., Greenberg, J., Kaplan, L. & Cahen, D. n- And p-type post-growth self-doping of CdTe single crystals. *Journal of Crystal Growth* **214–215,** 1155–1157 (2000).
28. Gessert, T. A. *et al.* Comparison of minority carrier lifetime measurements in superstrate and substrate CdTe PV devices. *IEEE Phot. Spec. Conf.* 001271–001274 (2011). doi:10.1109/PVSC.2011.6186189
29. Kino, G. S. & Corle, T. R. *Confocal Scanning Optical Microscopy and Related Imaging Systems*. (Academic Press, 1996).
30. Ippolito, S. B., Goldberg, B. B. & Ünlü, M. S. High spatial resolution subsurface microscopy. *Appl. Phys. Lett.* **78,** 4071–4073 (2001).
31. Hell, S., Reiner, G., Cremer, C. & Stelzer, E. H. K. Aberrations in confocal fluorescence microscopy induced by mismatches in refractive index. *J. Microsc.* **169,** 391–405 (1993).

Acknowledgments

Work at the Molecular Foundry was supported by the Office of Science, Office of Basic Energy Sciences, of the US Department of Energy under Contract No. DE-AC02-05CH1123. This material is based upon work supported by the Department of Energy under Award Numbers DE-EE0005332 and DE-EE0005953.

Author contribution statement

E.S.B., P.J.S., B.E.H., and C.H.P. formulated the research. E.S.B., E.T.H., J.R.G., P.J.S., B.E.H., and C.H.P. analyzed the data. E.S.B. constructed the two-photon microscopy system. E.S.B. and E.T.H. performed the optical experiments. T.K. and S.A. fabricated the InGaN quantum well samples. B.E.H., Z.Y., E.C.S. and E.D.B.-C. prepared the treated CdTe samples. S.T.C. and S.A. performed the cathodoluminescence measurements. All authors contributed to the manuscript.

Additional Information

Competing financial interests

The authors declare no competing financial interests.

Tables

	Fast lifetime component, τ_f	**Slow lifetime component, τ_s**
Untreated CdTe:		
1P	0.34 ns (100%)	N/A
2P surface	0.27 ns (86%)	0.73 ns (14%)
2P sub-surface (Δz=4.5μm)	0.49 ns (78%)	1.82 ns (22%)
Treated CdTe:		
1P	0.51 ns (98%)	5.4 ns (2%)
2P surface	0.23 ns (80%)	9.2 ns (20%)
2P transition (Δz=1.0μm)	0.45 ns (47%)	17.7 ns (53%)
2P sub-surface (Δz=3.4μm)	0.66 ns (6%)	73.0 ns (94%)

Table 1. Summary of 1P and 2P lifetime results on untreated and treated CdTe crystals. Lifetime values are a result of biexponential fits of time decay data. Relative weightings of the lifetime components are shown in parentheses.

Figures

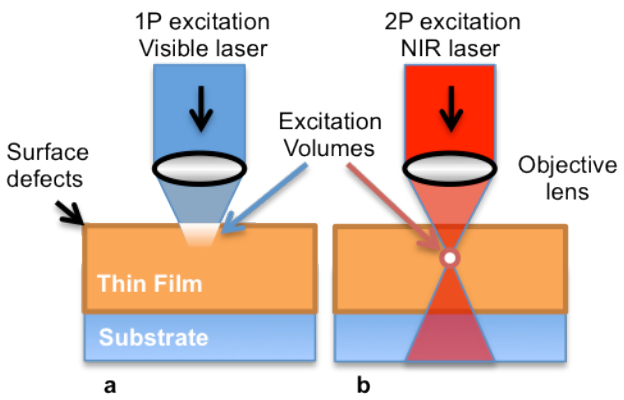

Figure 1. Schematic of one-photon versus two-photon excitation microscopy. (a) In traditional one-photon microscopy, incident light is absorbed predominantly at the surface following an exponential absorption profile. (b) Two-photon microscopy allows for direct optical excitation below the surface at the focus of an optical beam.

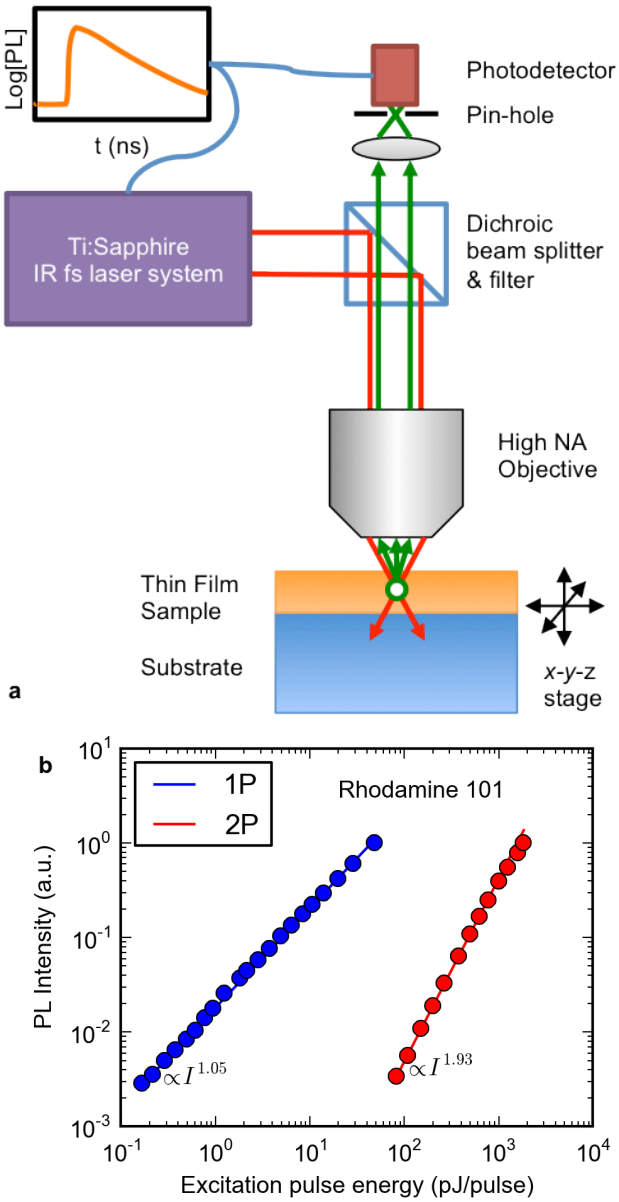

Figure 2. Two-photon excitation microscopy. (a) Schematic of the 2P-TRPL microscope used in this study. (b) One-photon and two-photon photoluminescence intensity dependence of Rhodamine 101 in ethanol with power-law fits.

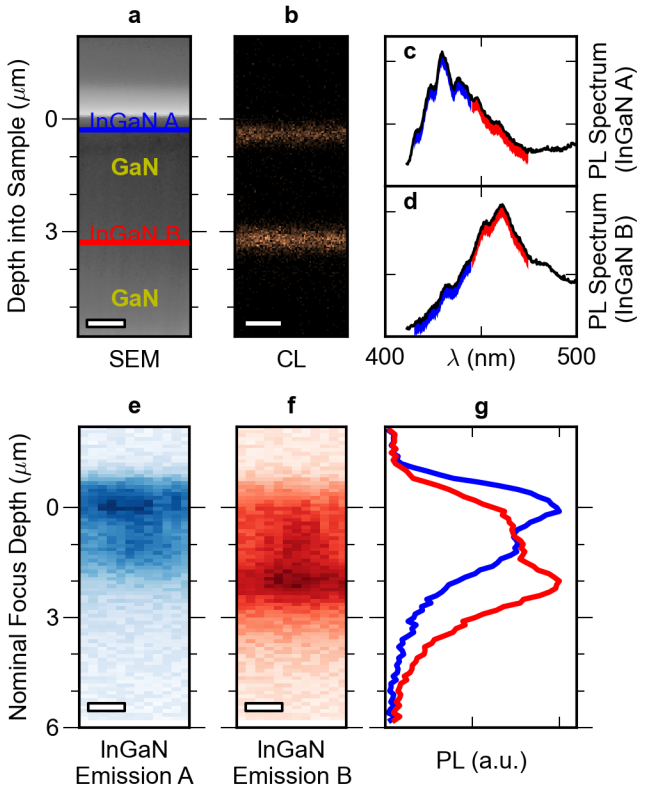

Figure 3. InGaN/GaN/InGaN double quantum well (QW) model system for confirmation of two-photon depth profiling ability. (a) Labeled scanning electron micrograph of the sample. Scale bar is 1µm. (b) Cathodoluminescence image of the same region of the sample as (a). (c) Representative emission spectrum of the top "A" InGaN QW. (d) Representative emission spectrum of the bottom "B" InGaN QW. (c-d) Blue and red highlights indicate spectral ranges used for the following figure panels. (e,f) Two dimensional depth cross-sectional maps of the emission of the InGaN QWs as measured by the 2P confocal microscope. Vertical axis is the nominal focus depth as measured by the motion of the sample stage. Horizontal axis is the lateral location of the sample stage. Scale bars are 1µm. (g) Normalized InGaN QW photoluminescence measured with the 2P confocal microscope as a function of nominal focus depth. Blue is InGaN "A" and red is InGaN "B".

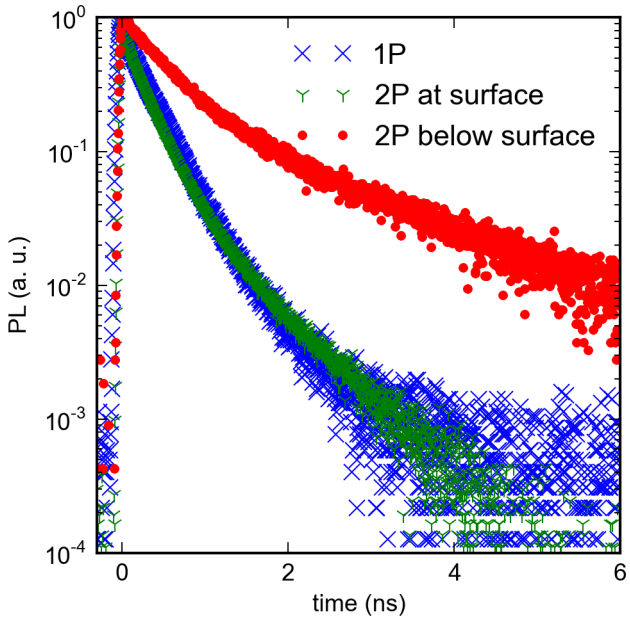

Figure 4. Comparison of one-photon and two-photon time-resolved photoluminescence on a single crystal CdTe sample. Blue curve indicates photoluminescence (PL) decay using one-photon excitation. Green curve shows PL decay when illuminating the surface of the sample with two-photon excitation. Red curve shows PL decay when focused at nominal focal depth of 3 μm into the film using two-photon excitation.

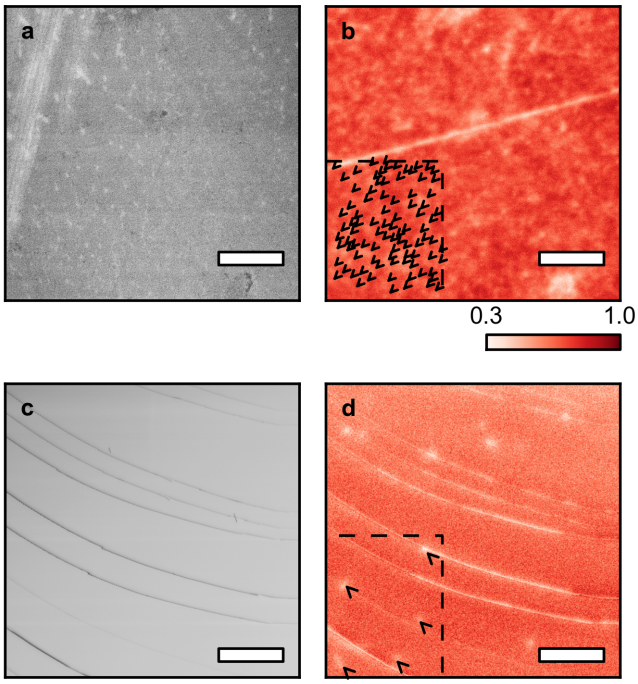

Figure 5 Cathodoluminescence (CL) of untreated CdTe crystal. All scale bars are 10 µm (a) Scanning electron micrograph (SEM) of the top surface of CdTe sample. (b) Associated CL image of the top surface. Arrows highlight examples of reduced emission sites due to surface defects within the dotted region. (c) Cross-sectional SEM of the cleaved CdTe sample. Long curved ridges are step edges introduced during cleaving process. (d) Associated CL image of the cross-section of the CdTe sample. Arrows again highlight defects within the dotted area. Note the reduced number of defects in (d) compared with (b). (b,d) colorbar shows the normalized CL intensity color scale.

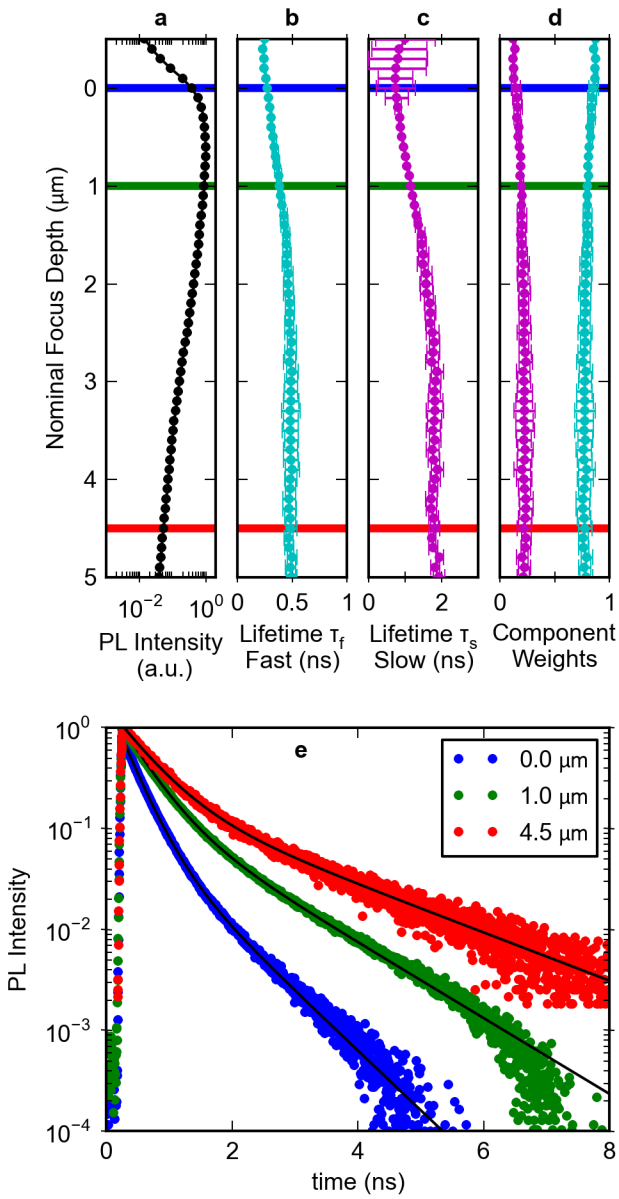

Figure 6. Depth-of-Focus two-photon TRPL of the untreated CdTe crystal. (a) Total photoluminescence intensity as a function of nominal focus depth (Δz) into sample as measured by the motion of the sample stage. (b,c) Results of a biexponential fit of PL decay as a function of nominal focus depth into the sample. (b) Short and (c) long lifetime components of the biexponential fit. (d) Relative weights of short (cyan) and long (magenta) components of the biexponetial fits. (e) Representative PL decay time traces at three different depths: at the surface and at nominal focus depths of 1.0 μm and 4.5 μm. Black lines are biexponential fits of the data.

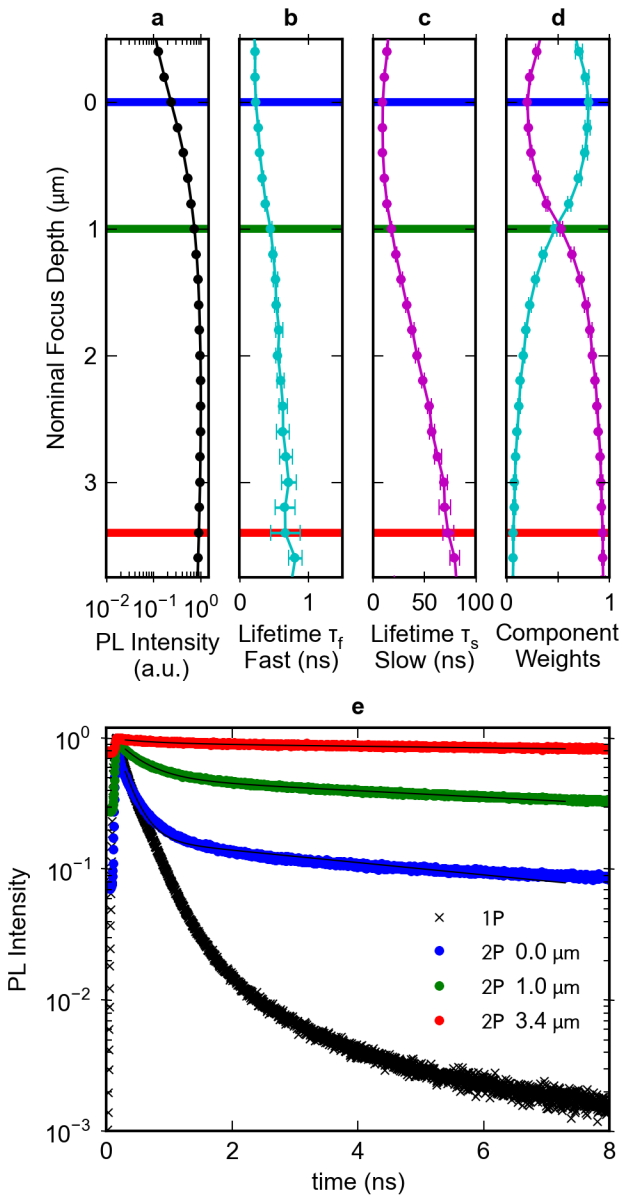

Figure 7. Depth-of-Focus two-photon TRPL of the treated CdTe crystal. (a) Total photoluminescence intensity as a function of nominal focus depth (Δz) into sample as measured by the motion of the sample stage. (b,c) Results of a biexponential fit of PL decay as a function of nominal focus depth into the sample. (b) Short and (c) long lifetime components of the biexponential fit. (d) Relative weights of short (cyan) and long (magenta) components of the biexponetial fits. (e) Representative 2P-TRPL decay time traces at three different depths: at the surface and at nominal focus depths of 1.0 μm and 3.4 μm. 1P-TRPL decay time trace is also plotted.

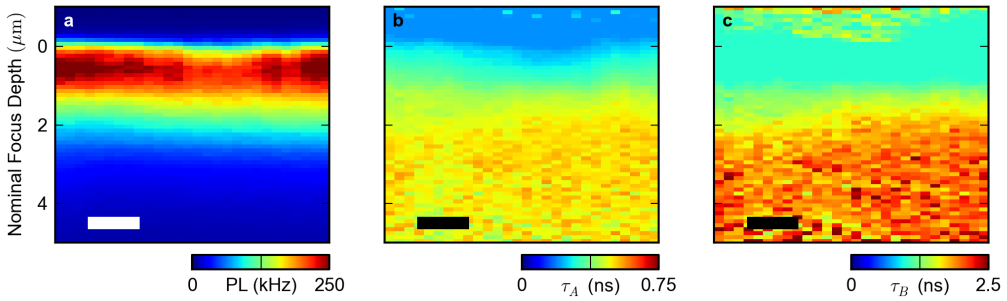

Figure 8. Cross-section depth maps of two-photon TRPL of CdTe. All scale bars are 1 µm. (a) Total photoluminescence intensity as a function of stage position. Vertical axis is the nominal focus depth as measured by the motion of the sample stage. Horizontal axis is the lateral location of the sample stage. (b,c) Results of a biexponential fit of PL decay at the same points shown in (a). (b) Fast and (c) slow lifetime components of the biexponential fit of lifetime curves.

Disclaimers.

This document was prepared as an account of work sponsored by the United States Government. While this document is believed to contain correct information, neither the United States Government nor any agency thereof, nor the Regents of the University of California, nor any of their employees, makes any warranty, express or implied, or assumes any legal responsibility for the accuracy, completeness, or usefulness of any information, apparatus, product, or process disclosed, or represents that its use would not infringe privately owned rights. Reference herein to any specific commercial product, process, or service by its trade name, trademark, manufacturer, or otherwise, does not necessarily constitute or imply its endorsement, recommendation, or favoring by the United States Government or any agency thereof, or the Regents of the University of California. The views and opinions of authors expressed herein do not necessarily state or reflect those of the United States Government or any agency thereof or the Regents of the University of California.

Copyright notice.

This manuscript has been authored by an author at Lawrence Berkeley National Laboratory under Contract No. DE-AC02-05CH11231 with the U.S. Department of Energy. The U.S. Government retains, and the publisher, by accepting the article for publication, acknowledges, that the U.S. Government retains a non-exclusive, paid-up, irrevocable, world-wide license to publish or reproduce the published form of this manuscript, or allow others to do so, for U.S. Government purposes.